



Sindh Univ. Res. Jour.

PALEOCENE THOLEIITIC VOLCANISM AND OCEANIC ISLAND ARC AFFINITIES OF THE CHAGAI ARC, BALOCHISTAN, PAKISTAN

R. H. Siddiqui, M. A. Khan*, M. Q. Jan** and I. A. Brohi***

Geosciences Laboratory, Geological Survey of Pakistan, Shahzad Town, Islamabad Pakistan
(Received 11th Jan. 2010 and Revised 06th April 2010)

Abstract

The main exposures of the Paleocene lava flows occur in an east-west trending subduction related magmatic belt known as Chagai Arc in the western part of Pakistan. The volcanism in this arc was initiated during the Late Cretaceous, which intermittently continued up to the Quaternary period. In the regional geotectonic context this arc belongs to the Tethyan Convergence Zone and was believed to have formed due to the northward subduction of Arabian Oceanic Plate below the southern margin of Afghan Micro plate and hence considered as an Andean type arc.

The Paleocene lava flows are mainly represented by amygdaloidal and nonamygdaloidal varieties of basalts (49.22-52.46 wt. % SiO₂) and basaltic-andesite (52.75-53.90 wt. % SiO₂). The main textures exhibited by these flows include hypocrySTALLINE porphyritic, cumuloPHYRIC, intersertal and subpilotaxitic. Large phenocrysts of augite and diopside (< 1 - 3 mm) and smaller of plagioclase (An₅₀₋₆₈) are embedded in a micro to crypto crystalline groundmass having the same minerals with devitrified volcanic glass.

The petrochemical studies show that these are mainly medium to low K oceanic island arc tholeiites. Their low Mg-number (41-55) and higher FeO (total)/MgO ratios (1.44-2.60) indicate fractionated nature of these lava flows. The trace element patterns show enrichment in LILE and depletion in HFSE relative to N-MORB. The primordial mantle-normalized trace element patterns show marked negative Nb anomalies with positive spikes on Ba and Sr which strongly confirm their island arc signatures, which is further supported by flate-slightly LREE enriched chondrite-normalized REE patterns. The Zr/Y versus Zr, and Cr versus Y studies, lowers Mg # and lower abundance of Ni and Co suggests that the parent magma of these rock suites was generated by about 15-30 % melting of depleted sub-arc mantle source, and fractionated in an upper level magma chamber en-route to eruption. These volcanics have lower average ⁸⁷Sr/⁸⁶Sr ratio (0.70446), which is more consistent with a depleted mantle source and closely correlate with oceanic island arcs rather than continental margin type arcs. The average trace element ratios including Zr/Y (2.25), Ti/V (15.47), Ti/Zr (160.17), Ba/Y (13.54), Th/Y (0.04) La/Yb_N (1.62), Ta/Yb (0.03), Th/Yb (0.24) of these volcanics are more consistent with oceanic island arc tholeiite rather than analogous rocks of the continental margins type arcs.

Keywords: Petrogenesis; Paleocene Volcanics; Oceanic Island Arc.

1. Introduction

The Chagai Arc is one of the economically most important mountain belts of Pakistan. Many important metal deposits including porphyry (Cu-Mo-Au), manto and vein type copper, stratiform and skarn type iron, volcanogenic gold-silver and sulphure, kuroko type lead-zinc-silver-copper are intimately associated with the magmatic rocks of this Arc (Siddiqui, 1996; Perello *et al.*, 2008). The Paleocene volcanic and Volcaniclastic rocks are generally well-exposed around Saindak, Maki Chah and Piran Ziarat areas within the lower middle part of the Juzzak Formation (Fig.1 and 2). The volcanic rocks include basaltic to andesitic lava flows, agglomerate, tuff and volcanic conglomerate.

In this paper, a detailed study of the Paleocene lava flows of the Chagai Arc, in terms of petrogenesis, is being presented to demonstrate their oceanic-arc setting.

The pioneer geological work in Chagai Arc was carried out by Vredenburg as early as in 1901. Hunting Survey Corporation (1960) conducted reconnaissance study and geological mapping of the entire Balochistan province on 1:253,440. During the seventies, many foreign geologists, including Sillitoe (1974), Nigell (1975), Dykstra (1978), Arthurton (1979) and Britzman (1979) visited the Chagai Arc. They considered the Chagai Arc as an Andean-type calc-alkaline magmatic belt, developed on the southern

* National Centre of Excellence in Geology University of Peshawar, Pakistan

** Quid-i-Azam University Islamabad, Pakistan

***Centre for Pure and Applied Geology, University of Sindh, Jamshoro, Pakistan

leading edge of the Afghan microplate, but no petrological or geochemical data were presented in support of the hypothesis. Ahmed (1984) also upheld a similar view on the basis of major elements chemistry of some acidic intrusive rocks. Siddiqui *et al.* (1986, 1987, 1988) and Siddiqui (1996) performed initial petrological studies, recorded both tholeiitic and calc-alkaline magmatism and proposed oceanic island Arc affinities for the Chagai Arc. Regional geological mapping of the Chagai Island Arc on 1:50,000 scale was started in 1960, and is still in progress by the Geol. Survey of Pak.

2. Material and Method

Appendix 1: Analytical Techniques.

a) Analyses of Major and Trace Elements: The major and trace elements were analyzed in the Geoscience Laboratory, Geological Survey of Pakistan, Islamabad, by X-ray fluorescence spectrometry (RIGAKU XRF-3370E). The sample powder (< 200 mesh), weighing 0.7 gram was thoroughly mixed with 3.5 gram of lithium tetra borate (flux). The analyses were carried out on 1: 5 rock powder and flux fused disks commonly known as glass beads. The samples thus obtained were analyzed by XRF using corresponding GSJ (Geological Survey of Japan) standard samples with every batch of ten samples. The results of analyses were then compared with the recommended values of USGS (United State Geological Survey) standard reference samples. A check of precision of the instrument was made using JA-3 standard sample (Govindaraju, 1989).

b) Analyses of Rare Earth Elements: The analysis of rare earth elements (REE) and Hf, Th, U and Ta was carried out in the GSJ on ICP-MS 2000 (YOKOGAWA, Japan). The 0.200 g sample (< 200 mesh) was weighed in a platinum dish and added 3 ml HClO₄, 4 ml HNO₃ and 5 ml HF. Heated on the hot plate at 200°C till complete evaporation. The dish was removed from the hot plate, cooled, washed and dried. The residue was added 5 ml 1: 1 HNO₃ and 5 ml water and gently heated on the hot plate till complete dissolution. The solution in the dish was cooled and filtered. The filtrate was transferred into a 100 ml measuring flask and added water up to 100 ml mark. The solution thus obtained was analyzed by ICP-MS, following Imai (1990) method, using JB-1 and JA-1 as standard samples (Govindaraju, 1989) and 1.5% HNO₃ as blank sample. The deduction limits of ICP-MS 2000 for all these elements are < 0.1 ppm. A check of precision of the instrument was made using JB-1 and JA-1 standard samples (Govindaraju, 1989).

c) Analyses of Sr Isotopes: The ⁸⁷Sr/⁸⁶Sr were determined by VG Micromass 3054R mass spectrometer at GSJ, Tsukuba, Japan. About 100 mg sample (< 200 mesh) was weighed in a platinum

crucible and added 3 ml ultra pure water and 10 ml super pure 40 % HF, and 5 ml HClO₄. The sample was decomposed on hot plate at 200°C till complete evaporation. It was added 2.5 N HCl and heated for 10 minutes. The sample was transferred in a small test tube and covered with scotch tap. Centrifuged the test tube samples at 3500 rpm for 10 minutes. Washed the cation exchange resin (CER) in the ion exchange column (IEC) by 2.5 N HCl. Transferred the test tube sample into IEC and passed it through CER. Washed twice the sample in IEC with 3 ml 2.5 N HCl. Passed through IEC 85 ml 2.5 N HCl (one hour) to separate Fe, K and other larger cations. Passed through IEC 20 ml 2.5 N HCl (half an hour) to separate Sr ions. This time smaller beakers were used to collect the sample. Transferred the sample into a small 5 ml beakers and heated the sample on hot plate till complete evaporation. Now mouth of the beaker was tightly closed with scotch tap. All the required samples and an additional GSJ standard sample (Govindaraju, 1989) were prepared following this method. The strontium isotopes in the samples were measured by VG Sector ionization Mass Spectrometer (Micromass 3054R) with dynamic four collector analysis. The ⁸⁷Sr/⁸⁶Sr ratios were normalized to ⁸⁶Sr/⁸⁸Sr = 0.1194. Repeated analyses of the NBS987 standard during the study gave 0.710256 ± 0.000015 (1 sigma). A check of precision of the instrument was made using JG-Ia standard sample (Govindaraju, 1989).

3. Geological Setting

The major part of the Chagai Arc is situated in the eruptive zone of western part of Pakistan; a small part of it also extends towards west in Iran and towards north in Afghanistan. This arc is about 500 km in length, 150 km in width and trends in an EW direction (Siddiqui *et al.*, 2005). The Arc is convex towards south and is terminated by the Chaman Transform Fault Zone in the east and Harirud Fault Zone in the west (Spector and Associates Ltd., 1981; Farah *et al.*, 1984).

The current tectonic setting of the region i.e. the presence of a north dipping oceanic subduction zone, an active accretionary prism followed by a magmatic arc (Chagai-Ras koh) comprising subduction related magmatism reflect a straightforward Andean type continental margin setting. Most of the previous workers have favored this tectonic setting of origin not only for the Quaternary volcanics but also for the volcanic rocks as old as Late Cretaceous (Stoneley, 1974; Stocklin, 1974; Sillitoe, 1978; Dykstra, 1978; Arthurton *et al.*, 1979; Farah *et al.*, 1984; Arthurton *et al.*, 1982; Kazmi and Jan, 1997). Siddiqui (1996) has contradicted this viewpoint and proposed oceanic island arc setting for the Late Cretaceous to Paleocene volcanics of the Chagai Arc.

The oldest rock unit of the Chagai Arc is the Cretaceous Sinjrani Volcanic Group (Fig.1, 2). The Group was invaded during Late Cretaceous to Pleistocene by Chagai intrusions, represented by several phases including granite, adamellite, granodiorite, tonalite, diorite and gabbro. Other rock formations exposed in the Chagai Arc are Humai Formation (Late Cretaceous), Juzzak/Rakhshani Formation (Paleocene), Saindak formation (Eocene), Robat Limestone (Early to Middle Eocene), Amalaf Formation (Oligocene), Dalbandin Formation (Miocene to Pleistocene), Buze Mashi Kok Volcanic Group (Miocene), Koh-e-Sultan Volcanic Group (Pliocene to Pleistocene) and semi to unconsolidated Subrecent and Recent deposits. The exposures of Paleocene Juzzak/Rakhshani formation are found throughout the Chagai Arc, while Paleocene lava flows are only observed in the western part of the Chagai Arc (Fig. 1 and 2). The generalized stratigraphic sequence in the Chagai Arc is presented in (Fig. 2).

The Paleocene volcanic and Volcaniclastic rocks are generally well-exposed around Saindak, Maki Chah (Fig. 1) and Piran Rud areas within the lower middle part of the Juzzak Formation (Fig. 3). The rocks include basaltic to andesitic lava flows, agglomerate, tuff and volcanic conglomerate.

Lava flows: Andesitic to basaltic lava flows are developed towards west of Maki Chah and east of Piran Ziarat (Fig. 1). In Maki Chah area the flows, which are about 320 m thick and extend for 12 km, are folded along with the adjacent strata of Juzzak Formation (Fig. 4A). They are greyish green to greenish black in colour, amygdaloidal in nature, moderately jointed and exhibit rugged physiography (Fig. 4B). The lavas are highly vesicular and vesicles are generally filled up with zeolite, calcite and chlorite. They are highly weathered, partially chloritized and porphyritic to microporphyritic in texture. Partially chloritized pyroxene and plagioclase represent the phenocrysts.

Another exposure of the lava flow occurs about 13 km southeast of Piran Ziarat, within the volcaniclastic sequence, trending NW-SE and dipping 40°SW. The lava flows are 60 meter thick and extends for 700 m (Fig. 4C). These lava flows are comparatively fresh, moderately jointed and show rugged physiography (Fig. 4D). They are basaltic in composition, non-amygdaloidal in nature and microporphyritic in texture. Pyroxenes with minor plagioclase constitute the phenocrysts.

Agglomerates: The agglomerates are dark green to black, thickly jointed, and show rugged physiography. They are mainly composed of rounded to subrounded

3 cm to 60 cm size fragments of basalt and andesite, embedded in a dark green to black tuffaceous matrix.

Tuffs: The tuffs have the same colour as agglomerates, are moderately jointed and show relatively smooth physiography. They are mainly composed of 1 to 1.5 cm size angular to sub-rounded fragments of volcanic rocks embedded in a compact and well-solidified volcanic ash.

Volcanic conglomerates: The volcanic conglomerates show rugged physiography, are grey to greenish grey in colour, and form upto 10 m thick beds. They are mainly composed of subangular to subrounded fragments of porphyritic andesites, basalts, tuffs and limestone, embedded in tuffaceous-sandy matrix of the same material. At places the conglomerates contain huge blocks (olistoliths) of limestone forming olistostrome deposits

3. Petrography

3.1 Piran Ziarat Lava Flows

Under the microscope, these rocks (sample Nos. Rp-1 to Rp-6) are hypocristalline, porphyritic, cumulophyric and intersertal in texture (Fig. 4E and F). Clusters of euhedral to subhedral phenocrysts of pyroxene and euhedral tabular crystal of plagioclase are embedded in a micro to cryptocrystalline groundmass of the same minerals. The phenocrysts to groundmass ratio is commonly 30: 70. Plagioclase occurs as euhedral to subhedral laths, which exhibit polysynthetic twinning according to albite and combined albite and Carlsbad laws. It is slightly fractured and shows minor argillization and sericitization. The anorthite content ranges from 50 to 65, which falls within labradorite, but a few of the plagioclase phenocrysts show much lower anorthite contents (An_{15-25}), due to albitization.

The clinopyroxene is represented by augite and minor diopside, which show euhedral to subhedral prismatic and eight sided sections. It occurs as phenocrysts and also occupies the interstices between the plagioclase crystals, imparting an intersertal texture to the groundmass. In the same Samples (Rp-5), small euhedral to subhedral crystals of basaltic-hornblende (oxy-hornblende) are also observed, which occur as phenocrysts as well as in the groundmass mineral (Fig. 4G). The basaltic-hornblende in groundmass commonly exhibits alteration rims of magnetite or hematite. Augite and diopside generally exhibit polysynthetic twinning and are partially altered into uralite and chlorite (Fig. 4H). Small euhedral and prismatic crystals of apatite are found as inclusions in the plagioclase. Subhedral to anhedral crystals of magnetite and titanomagnetite are found as inclusions in pyroxene and also scattered

throughout groundmass. Magnetite and titanomagnetite (Plates are often partially to completely replaced by hematite (martite).

3.2. Maki Chah Lava Flows

These rocks (Sample No.Mb-1 to Mb-4) show lower greenschist grade metamorphism, mainly represented by chloritization and argillization with minor epidotization and calcification. However, the original texture and relics of plagioclase and pyroxene crystals can be observed. These rocks show hypocrySTALLINE, porphyritic and intersertal textures and are amygdaloidal in nature. The phenocrysts to groundmass ratio is generally 25:75. Almost completely altered phenocrysts of plagioclase and clinopyroxene are embedded in a micro to cryptocrystalline groundmass of the same minerals.

Subhedral to anhedral crystals partially hematitized crystals of magnetite are scattered throughout the groundmass. The rocks are intensely vesiculated and the vesicles are generally filled with calcite, chlorite or zeolite.

4. Geochemistry

A total numbers of ten rock samples were collected from two localities of Paleocene volcanics from Chagai Arc six from Piran Ziarat area and four from Maki Chah area (Fig. 1). All the samples were analyzed for major and trace elements, alongwith rare earth elements (REE) for four samples from Piran Ziarat area and one from Maki Chah area. One sample from the Maki Chah area is also analyzed for Sr isotopes. The analytical techniques are given as Appendix 1 at the end of this paper.

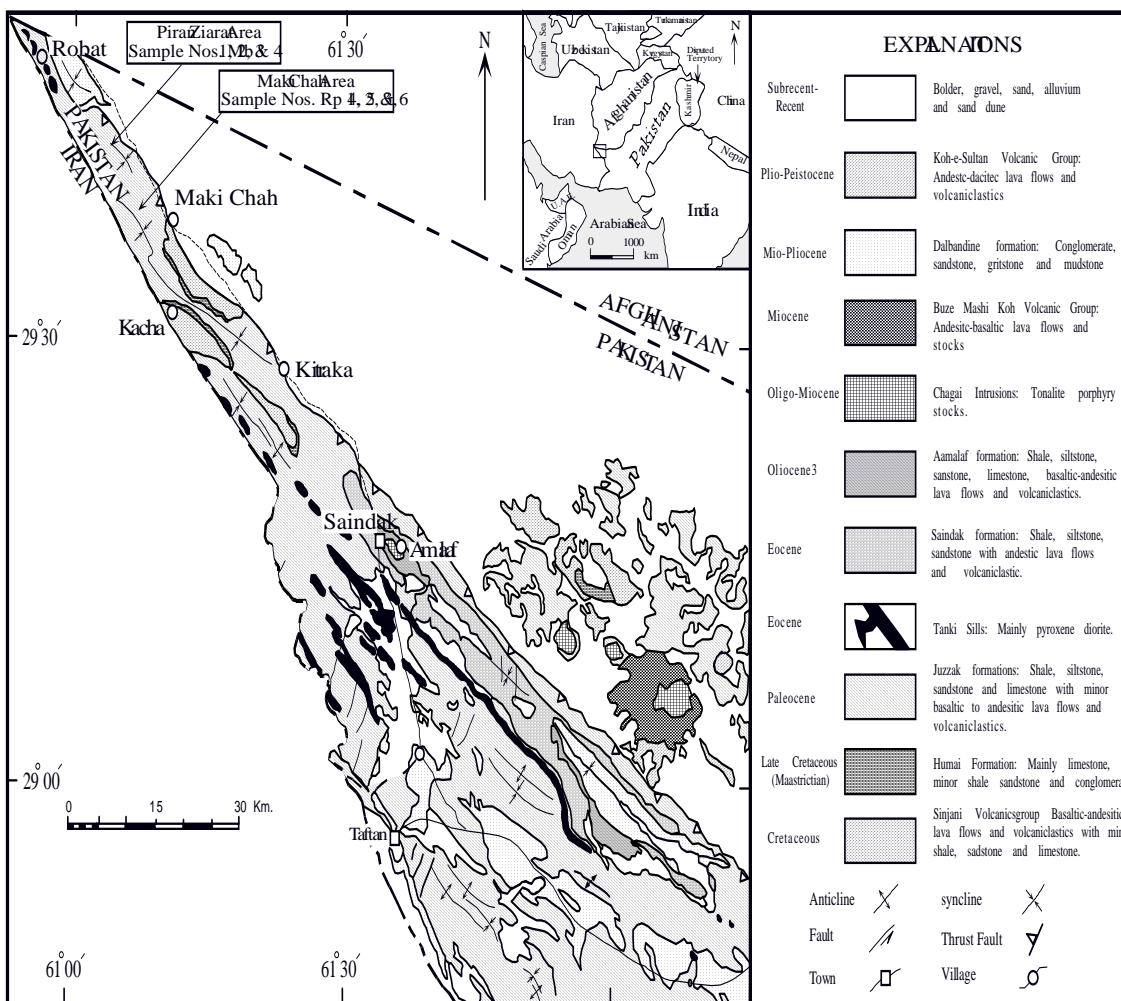


Fig. 1. Geological map of the western Chagai Arc, Balochistan, Pakistan. (modifies and reproduced after Bakr and Jackson, 1964; Siddiqui, 2004).

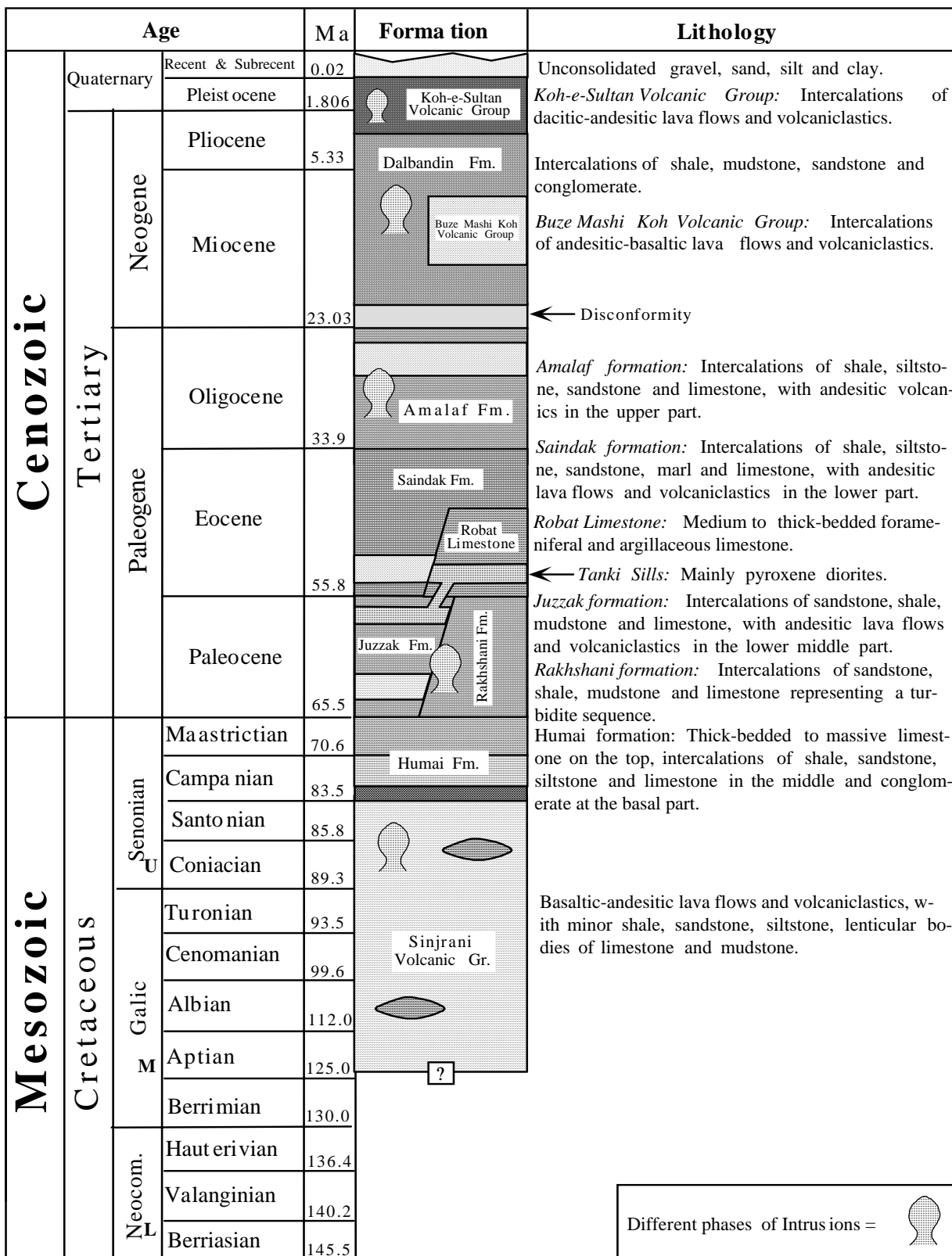


Fig. 2 Generalized stratigraphic sequence in the Chagai Arc (based on Jones, 1960; Siddiqui, 2004). The ages in the time scale are after Ogg *et al.* (2008).

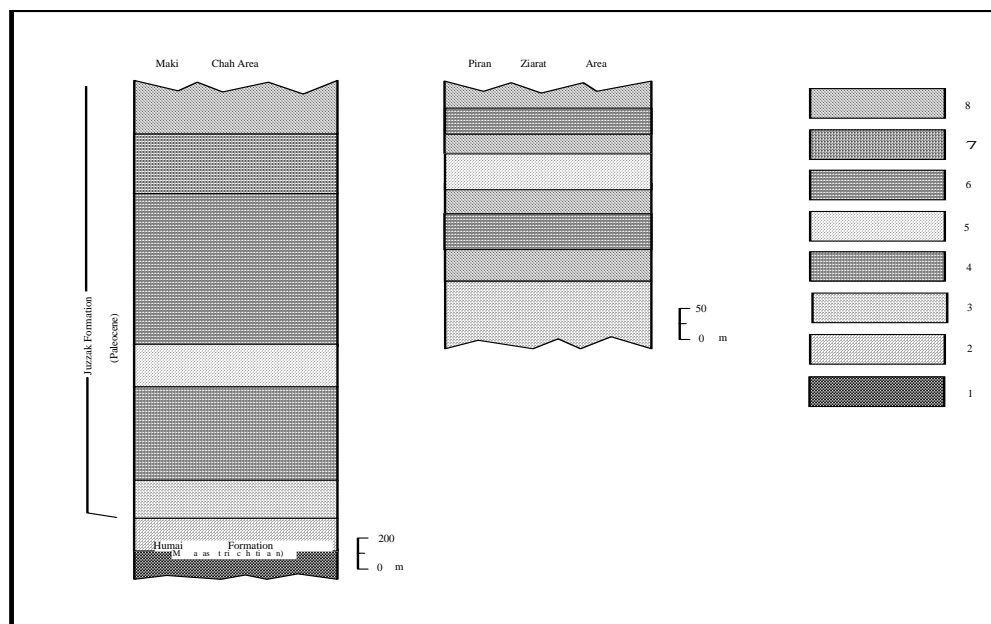


Fig. 3. Generalized internal stratigraphy in the Juzzak Formation. 1 represent conglomerate, 2 hippuritic limestone, 3 shale, 4 shale intercalated with limestone, 5 lava flow, 6 tuff intercalated with shale, 7 limestone and 8 conglomerate.

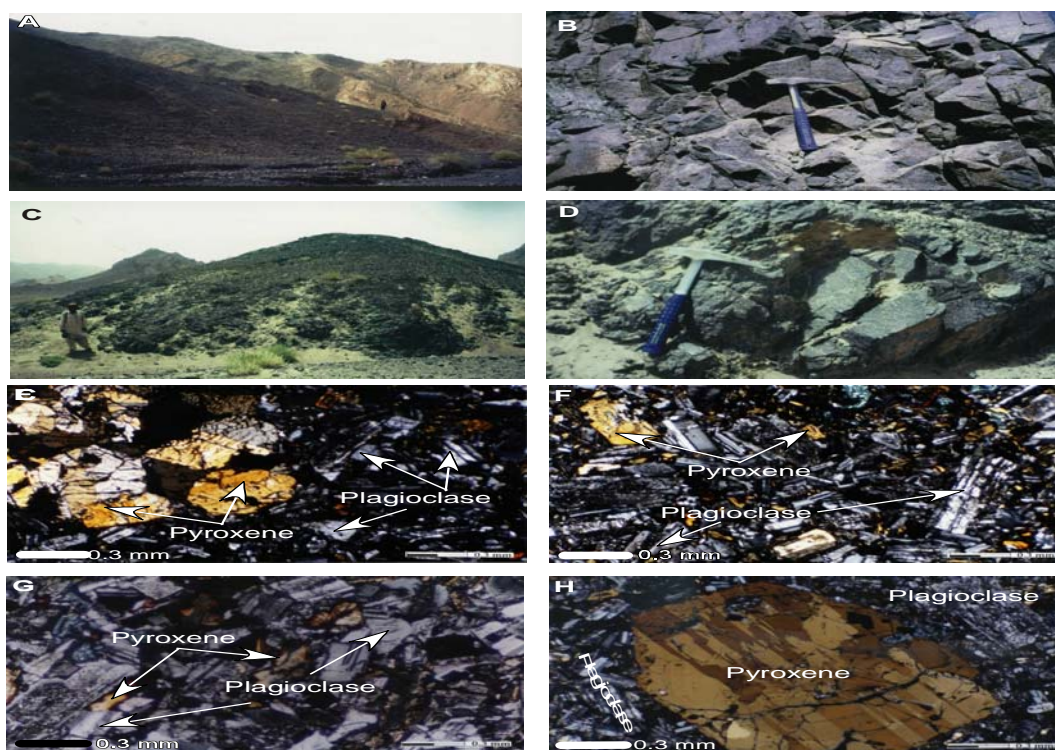


Fig. 4. (A) Massive lava flows (black) resting on the sedimentary sequence in the lower middle part of the Juzzak formation in Maki Chah area, western Chagai arc. View looking towards northeast, (B) A closer view of massive lava flows displaying intensely developed blocky joints in basaltic andesite of the Juzzak formation in Maki Chah area, western Chagai arc, (C) Massive lava flows (black) within volcaniclastic rocks in the lower middle part of the Juzzak formation in Piran Ziarat area, western Chagai arc, (D) A closer view of massive lava flows in Piran Ziarat area, (E) Photomicrograph of a basalt (Rp-2) exhibiting cumulophyric texture formed by the clustering of twinned phenocrysts of clinopyroxene crystals in a microcrystalline groundmass, which itself displays intersertal texture, (F) Another basalt (Rp-2) showing porphyritic and intersertal texture produced by the occurrence of small crystals of clinopyroxene within the interstices between the plagioclase crystals. On top left a marginally zoned phenocryst of augite with embayment of groundmass minerals, (G) Basalt (Rp-2) displaying intersertal texture formed by the occurrences of small prismatic and subhedral crystals of basaltic hornblende (rimmed by hematite) in interstices between the small plagioclase crystals. The plagioclase phenocryst on the lower left corner is marginally zoned and intensely sericitized and argillized, (H) Photomicrograph of another basalt (Rp-3) exhibiting fracturing and polysynthetic twinning in a phenocryst of clinopyroxene embedded in a microcrystalline groundmass having plagioclase, augite and volcanic glass. All photomicrograph are in crossed polarized light.

Bulk chemical analyses of the samples given in (Table 1) and Sr isotope data is presented in (Table 2). The major elements are recalculated on a volatile free basis, because some of the sample shows

loss on ignition up to 3.45 wt. % due to their low green schist grade metamorphic alteration as already mentioned in the section on petrography.

Table 1. Bulk chemistry of the Paleocene volcanics from the Chagai Arc.

| | Piran Ziarat Volcanics | | | | | | Maki Chah Volcanics | | | |
|------------------------------------|------------------------|--------|-------|-------|--------|-------|---------------------|--------|--------|-------|
| | Rp-4 | Rp-3 | Rp-5 | Rp-2 | R-6 | Rp-1 | Mb-1 | Mb-2 | Mb-3 | Mb-4 |
| SiO ₂ | 49.22 | 50.65 | 52.03 | 52.46 | 52.75 | 53.2 | 51.02 | 53.4 | 53.9 | 53.83 |
| TiO ₂ | 1.02 | 1.01 | 0.86 | 0.7 | 0.82 | 1 | 0.81 | 0.85 | 0.84 | 0.87 |
| Al ₂ O ₃ | 17.09 | 16.72 | 20.85 | 21.75 | 17.31 | 16.63 | 17.42 | 17.41 | 17.18 | 19.22 |
| Fe ₂ O ₂ | 11.64 | 11.4 | 9.01 | 8.23 | 12.18 | 11.41 | 11.51 | 11.81 | 11.31 | 9.75 |
| MnO | 0.19 | 0.16 | 0.18 | 0.18 | 0.16 | 0.18 | 0.2 | 0.15 | 0.13 | 0.15 |
| MgO | 7.19 | 6.81 | 4.78 | 4.37 | 5.59 | 6.93 | 4.03 | 5.41 | 5.41 | 3.76 |
| CaO | 9.36 | 9.51 | 5.01 | 5.1 | 7.94 | 9.49 | 13.42 | 7.82 | 7.27 | 9.37 |
| Na ₂ O | 3.39 | 3.02 | 4.49 | 4.25 | 3.01 | 3.22 | 1.22 | 2.36 | 3.18 | 2.89 |
| K ₂ O | 0.74 | 0.55 | 2.65 | 2.65 | 0.09 | 0.6 | 0.02 | 0.23 | 0.72 | 0.58 |
| P ₂ O ₅ | 0.17 | 0.15 | 0.15 | 0.15 | 0.05 | 0.16 | 0.04 | 0.06 | 0.05 | 0.11 |
| FeOt/MgO | 1.44 | 1.49 | 1.68 | 1.67 | 1.94 | 1.46 | 2.60 | 1.94 | 1.86 | 2.31 |
| Mg # | 55 | 54 | 52 | 52 | 48 | 55 | 41 | 48 | 49 | 44 |
| K ₂ O/Na ₂ O | 0.22 | 0.18 | 0.59 | 0.62 | 0.03 | 0.19 | 0.02 | 0.10 | 0.23 | 0.20 |
| Rb | 12 | 9 | 48 | 43 | 4 | 10 | 4 | 7 | 5 | 9 |
| Sr | 406 | 426 | 797 | 738 | 206 | 416 | 53 | 206 | 237 | 329 |
| Ba | 198 | 212 | 886 | 668 | 50 | 223 | 23 | 53 | 74 | 116 |
| V | 347 | 311 | 305 | 342 | 485 | 363 | 403 | 348 | 342 | 255 |
| Cr | 115 | 100 | 36 | 33 | 38 | 135 | 49 | 32 | 33 | 40 |
| Co | 41 | 43 | 30 | 43 | 33 | 42 | 32 | 41 | 43 | 20 |
| Ni | 34 | 31 | 21 | 6 | 9 | 35 | 6 | 9 | 6 | 11 |
| Zr | 63 | 49 | 72 | 45 | 18 | 61 | 21 | 19 | 20 | 55 |
| Y | 24 | 27 | 19 | 16 | 13 | 25 | 13 | 12 | 12 | 20 |
| Nb | 2 | 0.36 | 1 | 0.47 | 1 | 2 | 1 | 0.47 | 3.6 | 1 |
| Hf | 1.44 | 1.21 | — | 1.16 | — | 1.55 | — | 0.51 | — | — |
| Ta | 0.06 | 0.02 | — | 0.07 | — | 0.11 | — | 0.03 | — | — |
| Th | 1.19 | 1.06 | — | 0.73 | — | 1.15 | — | 0.18 | — | — |
| U | 0.33 | 0.29 | — | 0.28 | — | 0.42 | — | 0.07 | — | — |
| Sc | 44 | — | — | — | — | 45 | — | — | — | — |
| La | 6.92 | 5.6 | — | 4.39 | — | 9.95 | — | 1.00 | — | — |
| Ce | 13.65 | 12.67 | — | 11.03 | — | 20.17 | — | 2.84 | — | — |
| Nd | 10.52 | 9.44 | — | 7.58 | — | 12.4 | — | 2.77 | — | — |
| Sm | 2.88 | 2.68 | — | 2.11 | — | 3.31 | — | 1.14 | — | — |
| Eu | 1.03 | 0.93 | — | 0.91 | — | 1.04 | — | 0.53 | — | — |
| Gd | 3.54 | 3.4 | — | 2.78 | — | 3.63 | — | 1.30 | — | — |
| Er | 2.19 | 2.68 | — | 1.65 | — | 2.34 | — | 1.39 | — | — |
| Yb | 2.89 | 2.37 | — | 1.49 | — | 2.8 | — | 1.15 | — | — |
| ΣREE | 43.62 | 39.77 | — | 31.94 | — | 55.64 | — | 12.12 | — | — |
| Eu _N /Eu* | 0.99 | 0.95 | — | 1.16 | — | 0.92 | — | 1.34 | — | — |
| Ce _N /Ce* | 0.84 | 0.92 | — | 1.01 | — | 0.96 | — | 0.90 | — | — |
| (La/Yb) _N | 1.60 | 1.58 | — | 1.96 | — | 2.37 | — | 0.58 | — | — |
| (La/Ce) _N | 1.33 | 1.16 | — | 1.04 | — | 1.29 | — | 0.92 | — | — |
| (La/Sm) _N | 1.48 | 1.29 | — | 1.28 | — | 1.85 | — | 0.54 | — | — |
| (Ce/Yb) _N | 1.20 | 1.36 | — | 1.88 | — | 1.83 | — | 0.63 | — | — |
| La/Yb | 2.39 | 2.36 | — | 2.95 | — | 3.55 | — | 0.87 | — | — |
| Ce/Yb | 4.72 | 5.35 | — | 7.40 | — | 7.20 | — | 2.47 | — | — |
| Zr/Y | 2.63 | 1.81 | 3.79 | 2.81 | 1.38 | 2.44 | 1.62 | 1.58 | 1.67 | 2.75 |
| Zr/Nb | 31.50 | 136.11 | 72.00 | 95.74 | 18.00 | 30.50 | 21.00 | 40.43 | 5.56 | 55.00 |
| Ti/Zr | 96.98 | 123.47 | 71.54 | 93.18 | 272.89 | 98.20 | 231.05 | 268.00 | 251.60 | 94.75 |
| Ti/V | 17.61 | 19.45 | 16.89 | 12.26 | 10.13 | 16.50 | 12.04 | 14.63 | 14.71 | 20.44 |
| Th/U | 3.61 | 3.66 | — | 2.61 | — | 2.74 | — | — | — | — |
| Th/Yb | 0.41 | 0.45 | — | 0.49 | — | 0.41 | — | — | — | — |
| Ta/Yb | 0.02 | 0.01 | — | 0.05 | — | 0.04 | — | — | — | — |

FeOt = Total iron as FeO, Mg # = 100xMg / (Mg+Fe⁺²), SiO₂-P₂O₅ are in %, Rb-Yb are in ppm REE ratios with _N are chondrite Normalized (after Nakamura, 1974), REE with * are interpolated values (see text for details).

Table 2. Sr isotopic data of one sample from the Paleocene lava flows of the Chagai Arc.

| Sample No | Estimated Age | Rb/Sr | $^{87}\text{Sr}/^{86}\text{Sr}$ | $^{87}\text{Sr}/^{86}\text{Sr}$ (corrected: using Rb/Sr ratio and estimated age) |
|-----------|---------------|-------|---------------------------------|--|
| P-3a | 57.8 Ma | 0.021 | 0.70451 | 0.70446 |
| P-3b | 63.6 Ma | 0.021 | 0.70451 | 0.70446 |
| Average | | | | 0.70446 |

Sr isotopic ratios were measured by VG Sector Ionization Mass Spectrometer (Micromass 3054R) with dynamic four collector analysis. The $^{87}\text{Sr}/^{86}\text{Sr}$ ratios were normalized to $^{86}\text{Sr}/^{88}\text{Sr} = 0.1194$. Repeated analyses of the NBS987 standard during the study gave 0.710256 ± 0.000015 (1 sigma).

In total alkali-silica (TAS) diagram (Fig. 5), Le Bas *et al.*, (1986) two samples from Piran Ziarat Volcanics plot in trachybasaltic andesite field, one in basaltic andesite and three in basalt field.

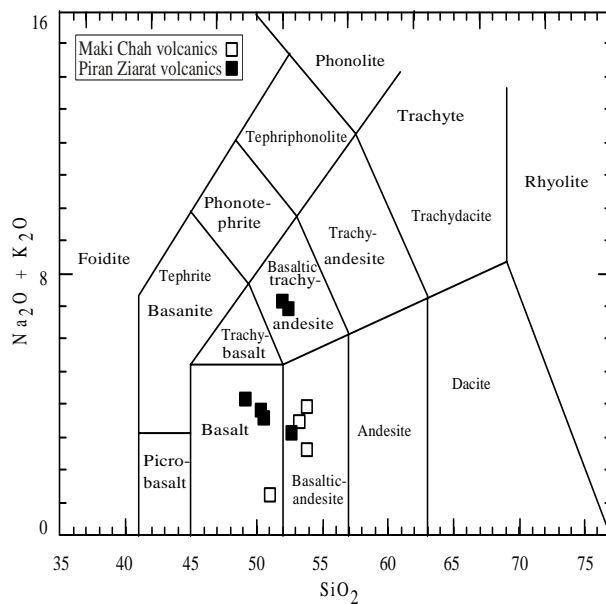


Fig. 5. Alkali versus SiO_2 plot (after Le Bas, *et al.*, 1986) for the Paleocene volcanic rocks from the Chagai Arc.

Of the Maki Chah Volcanics, one sample plots in basalt field, and the rest in basaltic andesite field. The higher values of K or total alkalis ($\text{Na}_2\text{O} + \text{K}_2\text{O}$ wt. %) may be attributed to submarine alteration, as suggested by Melson *et al.*, (1968) and Fyfe (1976). In order to verify whether the two samples from Piran Ziarat area are truly alkaline or not, the samples of the Paleocene volcanics are again plotted in Zr/TiO_2 versus Nb/Y diagrams (Winchester and Floyd, 1977) which reveals that all the samples are non-alkaline in nature. In this diagram all the samples are plotted in non-alkaline fields (Fig. 6).

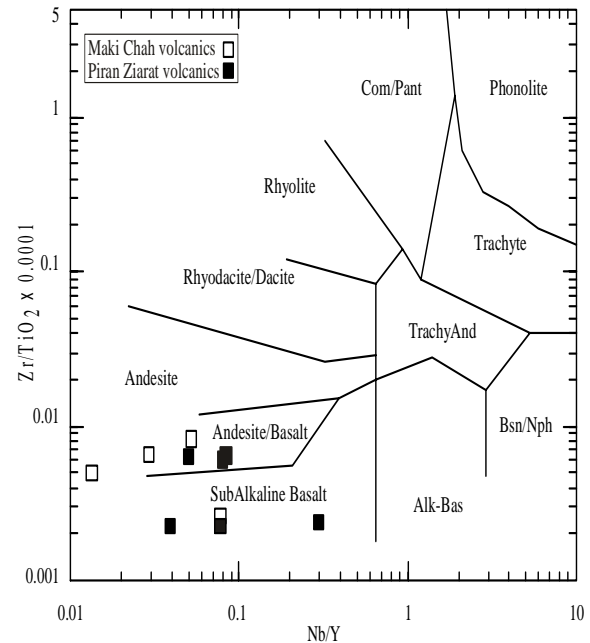


Fig. 6. Zr/Ti versus Nb/Y plot (after Winchester and Floyd, 1977) for the Paleocene volcanic rocks from the Chagai Arc.

The rock classification based on TAS diagram appears to be inappropriate, particularly for Piran Ziarat Volcanics and suggests that total alkalis of these Volcanics have been affected by post-magmatic alteration processes. The CaO contents in the rocks are also greatly variable; some of the sample contain up to 13 wt. % CaO due to partial replacement of some minerals by calcite and its presence as amygdales and veinlets. Similarly, original contents of SiO_2 , Al_2O_3 and other major elements may have been changed due to alteration processes and fillings of certain minerals like chlorite, chalcedony and zeolites in the vesicles. Therefore it is suggested that merely use of major elements is not appropriate and reliable for classification and petrogenetic evaluation for these rocks.

The Piran Ziarat Volcanics have lower (1.44-1.94) FeOt/MgO ratios as compared to Maki Chah (1.94-2.60) Volcanics (Table 1). The Mg # ($100 \times \text{Mg}/\text{Mg} + \text{Fe}^{2+}$) is also higher (48-55) in Piran Ziarat Volcanics relative to the Maki Chah Volcanics (41-49). Higher concentrations of MgO wt. % and higher values of Mg # and lower values of FeOt/MgO suggests that the Piran Ziarat Volcanics are more depleted in nature and probably formed by higher degree of partial melting of the magmatic source.

4.1. Trace Element Abundances

Large Ion Lithophile Elements (LILE): Both the Volcanics generally have higher concentrations of LILE as compared to high field strength elements (HFSE). The Piran Ziarat Volcanics generally show overlapped progressive increase of Rb, Ba, Sr, Th and U relative to those of Maki Chah Volcanics (Table 1), which suggests that former Volcanics are more fractionated in nature.

High Field Strength Elements (HFSE): The Piran Ziarat Volcanics generally show overlapped progressive increase for Ti, Zr and Y, Hf relative to those of Maki Chah volcanics, whereas Nb and Ta show reversed behavior. **Spider Diagrams:** The spider diagrams or multi-elements diagram are generally used to study the behavior of incompatible trace elements in the rocks and to constrain their source regions, with reference to primordial mantle or N-MORB compositions. For this purpose all the samples from Paleocene volcanic rocks from the Chagai arc are plotted in primordial mantle normalized spider diagram (Fig. 7) with an average trace element spider plot of N-MORB in the same plot for comparison (both normalizing and average values are after Sun and McDonough, 1989).

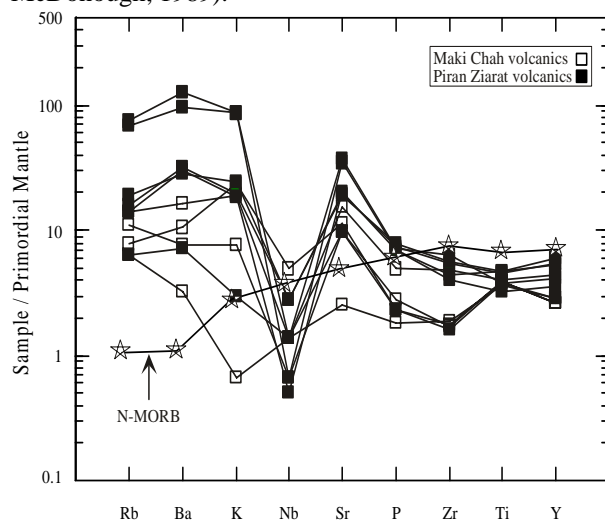


Fig. 7. Primordial mantle normalized spider diagram for the Paleocene volcanic rocks from the Chagai Arc. The starred pattern is for average N-MORB. Average N-MORB and normalization values are after Sun and McDonough (1989).

The incompatible trace element patterns in this diagram exhibit enrichment of LILE elements and depletion in HFS elements relative to N-MORB. The patterns show marked negative Nb anomalies and positive spikes on Sr and Ba, which are consistent with the Island Arc Volcanics. These patterns also show enrichment of LILE in Piran Ziarat Volcanics relative to Maki Chah Volcanics. The Piran Ziarat Volcanics also show overlapped increase of all HFSE except Nb, which exhibit overlapped decrease. The spider pattern and (Table 1) also exhibit enhanced LILE/HFSE ratios (Rb/Y, Ba/Y and Ba/Zr) in the Piran Ziarat Volcanics, which are suggestive of their more fractionated nature.

4.2. Compatible Elements

Cr, Ni and Co in the Piran Ziarat Volcanics are generally more enriched in these elements, which is an evidence for their more depleted nature.

4.3. Rare Earth Elements (REE)

The rare earth elements (La, Ce, Nd, Sm, Eu, Gd, Er and Yb) were analyzed for four samples (Rp-1, 2, 3, 4 and Mb-2) from Piran Ziarat Volcanics and one (Mb-1) from Maki Chah volcanics. Both the volcanics have higher concentrations of light rare earth elements (LREE) as compared to heavy rare earth elements (HREE). The total REE (ΣREE) concentrations in basaltic andesite with similar SiO_2 are much higher (55.64) in Piran Ziarat volcanics relative to those in Maki Chah Volcanics (12.12). The Piran Ziarat volcanics also have higher normalized LREE/HREE ratios ($\text{La}_N/\text{Yb}_N = 1.58$ to 2.37 and $\text{Ce}_N/\text{Yb}_N = 1.20$ - 1.88) as compared to the single analyzed sample from the Maki Chah volcanics (0.90 and 0.58, respectively). Similarly the Piran Ziarat Volcanics have a higher but narrow range of La_N/Ce_N (1.33-1.29), La_N/Sm_N (1.48-1.85) ratios, as compared to the single analyzed sample from the Maki Chah Volcanics (0.54 and 0.63) respectively.

The measured Eu anomalies (Eu_N/Eu^*), which are calculated (Taylor and McLennan, 1985) by dividing the chondrite normalized (Eu_N) values and the interpolated (Eu^*) values [$\text{Eu}_N/\text{Eu}^* = \text{Eu}_N/\sqrt{(\text{Sm}_N \times \text{Gd}_N)}$] are also determined for these volcanic. All the samples, except one (Rp-2), exhibit negative (<1) Eu anomalies, which are consistent with plagioclase fractionation during differentiation. Similarly measured Ce anomalies (Ce_N/Ce^*), which are calculated by dividing the chondrite normalized (Ce_N) values with the interpolated (Ce^*) values [$\text{Ce}_N/\text{Ce}^* = \text{Ce}_N/\sqrt{(\text{La}_N \times \text{Nd}_N)}$] and also determined for these volcanics. All the samples exhibit negative (<1) Ce anomalies except one sample (Rp-2). The negative Ce anomalies indicate involvement of fluids generated by the dehydration of pelagic sediments in the subducted slab (Gill, 1981) and are also noted in many other island arc volcanic rock suites including Japan Arc (Masuda, 1968),

Solomon island Arc (Jakes and Gill, 1970) and Mariana Arc (Hole *et al.*, 1984).

Chondrite Normalized REE Diagrams: Chondrite normalized REE diagrams are generally prepared to determine the behavior of REE in the rocks and to constrain their source compositions, with reference to normalized chondritic values.

Chondrite normalized REE diagrams (**Fig. 8**) of Paleocene volcanic rocks of the Chagai arc show enrichment of LREE patterns for Piran Ziarat as compared to average N-MORB REE pattern (after Sun and McDonough, 1989). The HREE show variable depletion as compared to average N-MORB.

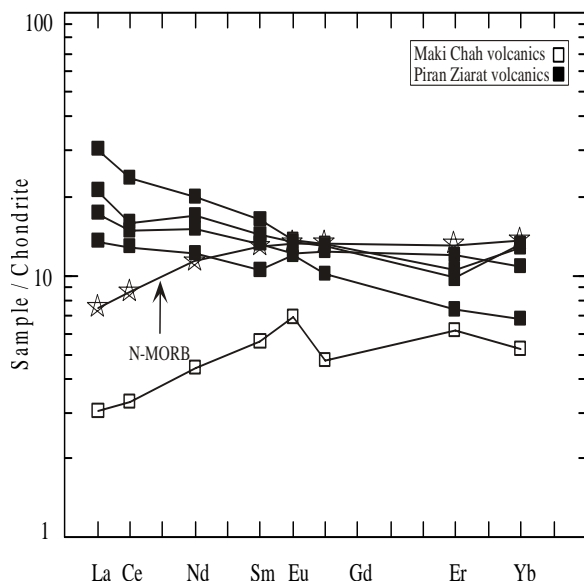


Fig. 8. Chondrite normalized REE diagram for the Paleocene volcanic rocks from the Chagai Arc. The starred pattern is for average N-MORB. Average N-MORB values are after Sun and McDonough (1989), whereas normalization values are after Nakamura (1974).

All the samples except one (Rp-2) show negative Ce anomalies, which indicate small amount of subducted pelagic sediments in the source (Hole *et al.*, 1984). Similarly, all the samples, except Rp-2, show negative Eu anomalies, which are generally linked with plagioclase fractionation during magmatic differentiation. The Rp-2 shows accumulation of plagioclase during differentiation.

4.6. $^{87}\text{Sr}/^{86}\text{Sr}$ isotope ratios:

One least altered sample from Piran Ziarat Volcanics (RP-3) was analyzed for $^{87}\text{Sr}/^{86}\text{Sr}$ isotope ratio (Table 2). The $^{87}\text{Sr}/^{86}\text{Sr}$ isotope ratio determined for this sample is 0.70446. This ratio is less than the reported ratio for Bulk Earth (0.7052). The magmas with $^{87}\text{Sr}/^{86}\text{Sr}$ ratios less than the Bulk Earth value are considered to be derived from a depleted mantle source (Wilson, 1989).

In (Table 3), average trace element chemistry of the Paleocene volcanic rocks of the Chagai arc is compared with average oceanic island Arc (Mariana and Tonga Arcs) and continental margin type (Andean type) Arcs including Andes, Java and New Guinea Arcs. This comparison shows close affinities of volcanic rocks of Chagai arc with oceanic island arcs rather than continental margin type Arcs (**Table 3**).

5. Results and Discussion

5.1. Petrogenesis Nature of Parent Magma

The criteria generally used to determine whether the basaltic rocks occurring an area represent the primary melts from the mantle peridotite source or these are the product of fractionated liquids, are:

- The presence of mantle peridotite (lherzolite) xenoliths within the basaltic volcanics series.
- The high magnesium number ($\text{Mg \#} = \text{Mg}/\text{Mg} + \text{Fe}^{2+}$) and low FeO/MgO ratios.
- Higher contents of compatible elements (Ni, Cr and Co).

No mantle lherzolite xenolith is encountered from Paleocene volcanic rock assemblage of the Chagai arc. The Mg # in Piran Ziarat and Maki Chah basalts to basaltic-andesites range from 48 to 55 and 41 to 49 respectively. The Ni (6-35 ppm), Cr (32-135 ppm) and Co (20-43 ppm) contents in both the volcanic groups are well below the values just mentioned (Table 1). Therefore, it is concluded that magmas of these rocks have not been directly derived from an upper mantle peridotite source but have undergone fractionation en route to eruption; most probably in an upper level magma chamber.

As already mentioned the Piran Ziarat volcanics have higher values of Mg #, Cr, Ni and Co and are fractionated from a magma derived from a more depleted mantle source region as compared to their Maki Chah counterparts. This is further supported by lower values of Ti/Zr and Ti/V ratios (Table 1).

The trace element ratios (Table 1) including Zr/Y, Ti/V, Zr/Nb, Ti/Zr, in both the volcanic group and Ta/Yb, Th/Yb and La/Yb in Piran Ziarat Volcanic are close to the reported values (Gill, 1981; Shervais, 1982; Wilson, 1989) of these ratios in the volcanic rocks of oceanic island arcs rather than those found in the similar rocks of continental margin type or Andean type Arcs.

5.2. Tectonic Setting

SiO_2 versus FeO/MgO plot (Miyashiro, 1974) reveals that all the rocks are tholeiitic in nature

Table 3. A comparison of average trace element chemistry of the Paleocene volcanic rocks of the Chagai Arc with some arc related Volcanic rocks of the world.

| | Oregon (Andes) USA | | Mariana Arc 1 | | | Andes Arc 2 | | | Tonga Arc 3 | | Java Arc 4 | New Guinea Arc 5 | |
|----------|--------------------|----------------------|---------------|--------------|----------------------|----------------|-----------|---------------------|-------------|----------------------|-------------|----------------------|----------------------|
| Elements | Basalt Th | Basaltic-andesite Th | Andesite Th | Basalt Th-CA | Basaltic-andesite CA | Andesite Th-CA | Basalt CA | Basalticandesite CA | Andesite CA | Basaltic-andesite Th | Andesite Th | Basaltic-andesite Th | Basaltic andesite Th |
| Rb | 23.20 | 7.00 | 67 | 14 | 12.67 | 12.67 | 50 | 45 | 75 | 6 | 9 | 50 | 25 |
| Sr | 484.00 | 278.80 | 660 | 303 | 311 | 378 | 608 | 644 | 648 | 235 | 220 | 605 | 810 |
| Ba | 397.40 | 103.20 | 1200 | 176 | 259 | 348 | 345 | 676 | 886 | 100 | 145 | 690 | 250 |
| V | 341.60 | 358.60 | 125 | 290 | 238 | 186 | 187 | 220 | 125 | 310 | 360 | 260 | 178 |
| Cr | 66.60 | 55.60 | 10 | 18 | 60.33 | 23.67 | 68 | 202 | 48 | 15 | 16 | 8 | 9 |
| Co | 37.80 | 35.80 | 15 | 49 | 45.67 | 31.33 | 30 | 31 | 19 | 28 | 30 | 18 | — |
| Ni | 19.60 | 14.00 | 16 | 12 | 10.33 | 10.33 | 58 | 67 | 39 | 13 | 4 | 3 | 6 |
| Zr | 50.00 | 34.60 | 19 | 59 | 71.33 | 70.6 | 162 | 179 | 195 | 28 | 21 | 98 | 81 |
| Y | 19.80 | 16.40 | 230 | 20 | 24.33 | 24 | 30 | 25 | 12 | 17 | 18 | 25 | 17 |
| Nb | 0.97 | 1.61 | 15 | 0.5 | 0.73 | 1.1 | — | 13 | — | 0.6 | 1.5 | 5 | 4 |
| Hf | 1.27 | 1.03 | 5 | — | — | — | 2.9 | 3.67 | 5.46 | 0.8 | 0.7 | 3.4 | 2.2 |
| Ta | 0.04 | 0.07 | 6.4 | — | — | — | — | — | — | 0.2 | — | — | — |
| Th | 0.99 | 0.67 | — | — | — | — | — | — | — | — | 0.6 | 8.1 | 1.3 |
| U | 0.30 | 0.25 | 36 | — | — | — | — | — | — | — | 0.3 | — | — |
| Cu | — | — | — | 130 | 91.67 | 103 | 30 | 49.6 | 40 | 145 | 240 | 38 | 46 |
| La | 5.64 | 5.48 | — | 17.43 | 21.8 | 30.6 | 16.3 | 24.6 | 38 | 1.8 | 3.0 | 22 | 11 |
| Ce | 12.45 | 11.51 | — | 13.87 | 18.0 | 25.3 | 41.6 | 51.3 | 66.8 | 4.7 | 6.9 | — | 24 |
| Nd | 9.18 | 7.59 | — | 14.21 | 17.17 | 23.33 | — | — | — | — | — | — | Nd |
| Sm | 2.56 | 2.23 | — | 12.33 | 15.57 | 20.37 | — | — | — | — | — | — | Sm |
| Eu | 0.96 | 0.79 | 1.9 | 11.60 | 13.7 | 17.1 | — | — | — | — | — | — | — |
| Gd | 3.24 | 2.47 | 48 | 10.50 | 14.23 | 18.03 | — | — | — | — | — | — | — |
| Er | 2.17 | 1.87 | 12.10 | 6.37 | 9.87 | 12.9 | — | — | — | — | — | — | — |
| Yb | 2.25 | 1.98 | 26.09 | 5.37 | 8.57 | 11.2 | 2.29 | 2.32 | 1.94 | 1.5 | 1.3 | 3.1 | 1.7 |
| Ti/V | 15.65 | 15.28 | 15.33 | 16.36 | 19.16 | 25.81 | 36.58 | 34.64 | 45.60 | 11.03 | 9.5 | 16.85 | 27.30 |
| Zr/Y | 2.53 | 1.96 | 18.95 | 2.95 | 2.93 | 2.94 | 5.23 | 7.04 | 15.98 | 1.65 | 1.75 | 3.92 | 4.76 |
| Ti/Zr | 123.24 | 197.09 | 37.37 | 80.34 | 63.92 | 67.99 | 42.22 | 42.57 | 29.23 | 122.14 | 162.86 | 44.69 | 60 |
| Zr/Nb | 71.27 | 29.90 | — | 118 | 97.71 | 64.18 | — | 14.32 | — | 46.67 | 14 | 19.60 | 20.25 |
| La/Yb | 2.57 | 2.21 | 3.37 | 5.37 | 2.54 | 2.73 | 7.12 | 10.60 | 19.49 | 1.2 | 2.31 | 7.10 | 6.47 |
| Ce/Yb | 5.82 | 4.84 | — | 2.58 | 2.10 | 2.26 | 2.55 | 22.11 | 34.43 | 3.13 | 5.31 | — | 14.12 |
| Ta/Yb | 0.02 | 0.03 | — | — | — | — | — | — | — | — | — | — | — |
| Th/Yb | 0.45 | 0.28 | — | — | — | — | — | 2.61 | — | 0.03 | 0.43 | — | 0.76 |

The values in column 1 are after Woodhead (1988), in 2 are after Ewart (1982), Oregon and the data in 3 - 5 are after Gill, (1981), SiO₂-P₂O₅ are in %, Rb-Yb are in ppm. Th & CA represent tholeiitic and calc-alkaline.

(Fig. 9A). The tholeiitic parentage and island Arc character of Paleocene Volcanics are further confirmed by plotting the samples in various discrimination diagrams, including, TiO₂-MnO-P₂O₅ plot (Mullen, 1983), Ti-Zr-Y plot (Pearce and Cann, 1973), Nb-Zr-Y plot (Meschede, 1986), Ti-Zr plot

(Pearce and Cann, 1973) shown in (Fig. 9B to E), respectively. The plots in Fig. 9B to E does not clearly discriminate island arc tholeiites and mid-oceanic ridge tholeiites; hence samples are again plotted in Ti versus V diagram (Shervais, 1982). This plot (Fig. 9F) clearly distinguishes and differentiates between island Arc

tholeiites (low-K tholeiite) and Ocean floor tholeiites. The plots in these diagrams strongly confirm tholeiitic parentage and oceanic island Arc character of the Paleocene volcanic rocks of the Chagai Arc.

To ascertain whether the Paleocene volcanic rocks of the Chagai Arc were erupted in an oceanic island Arc environment or produced in a continental margin type arc settings all these sample are plotted in

Zr/Y versus Zr diagram (Pearce, 1983), which clearly distinguishes the oceanic island arcs and continental margin type arcs (Fig. 9G). A plot of various samples from the Paleocene volcanic rocks in Th/Yb-Ta/Yb diagram (Pearce, 1983) further confirms its oceanic island Arc affinity and suggests that the parent magmas of these volcanics were generated by the partial melting of a depleted mantle source (Fig. 9H).

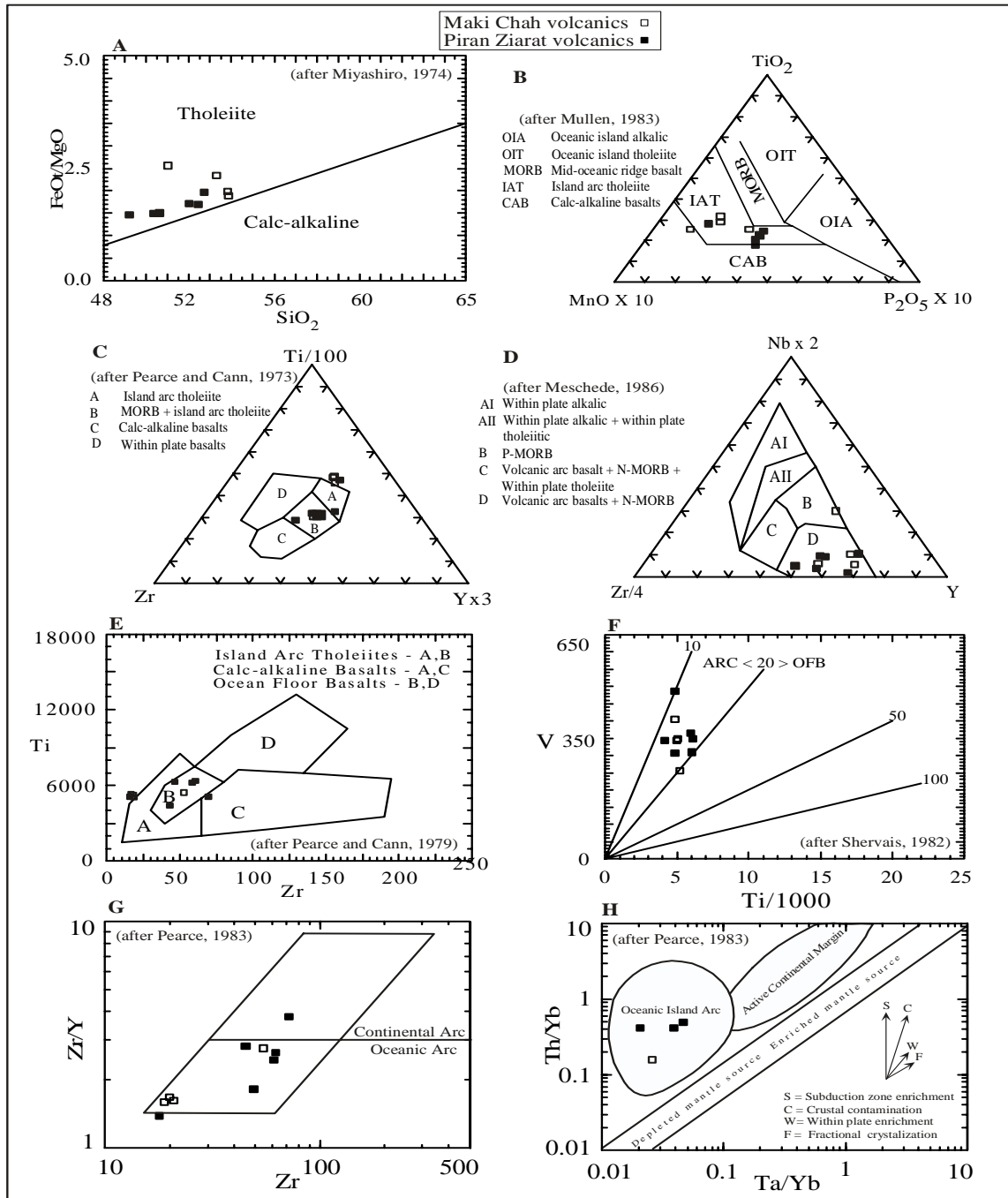


Fig. 9

Fig. 9 A to H. Various tectonomagmatic discrimination diagrams for the Paleocene Volcanic rocks from the Chagai Arc.

As already mentioned that the spider patterns (Fig. 7), which exhibit positive spikes generally on Ba and Sr, with marked negative anomalies on Nb, strongly confirm their island arc signatures (Pearce, 1982; Wilson 1989; Saunders and Tarney, 1991). The marked negative Nb anomalies are explained by retention of this element in the residual mantle source during its partial melting (Pearce, 1982; Wilson, 1989). The positive spikes of certain elements are generally considered to have formed by incorporation of these elements in the source from the subducting slab (Pearce, 1982; Wilson, 1989).

5.3. Nature of the Source of Parent Magma:

The Zr versus Zr/Y diagram (Fig. 10) provides useful information about the nature of source, degree of partial melting and fractionation etc. Plot of various rock samples from the Paleocene volcanic rocks from the Chagai Arc in this diagram

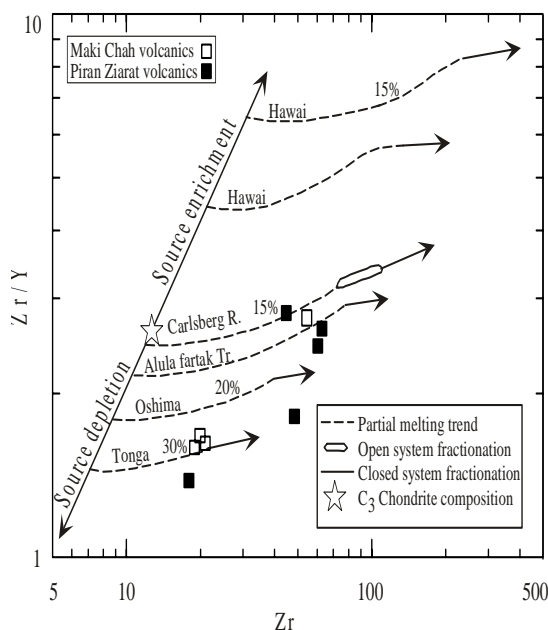


Fig. 10. Zr versus Zr/Y plot (Pearce and Norry, 1979) for the Paleocene volcanic rocks from the Chagai Arc.

(Pearce and Norry 1979) indicate that these rocks are fractionated from 15 to 30 % partially melted depleted mantle source. Plot (Fig. 11) in Cr versus Y diagram (Pearce, 1982), which is also designed for the estimation of degree of partial melting and fractionation exhibits higher degree of Partial melting (23 - 40%) of mantle source.

The $^{87}\text{Sr}/^{86}\text{Sr}$ ratios are also used to ascertain the mantle source of parent magma as these ratios remain unchanged or exhibit very little deviation during partial melting and fractionation processes

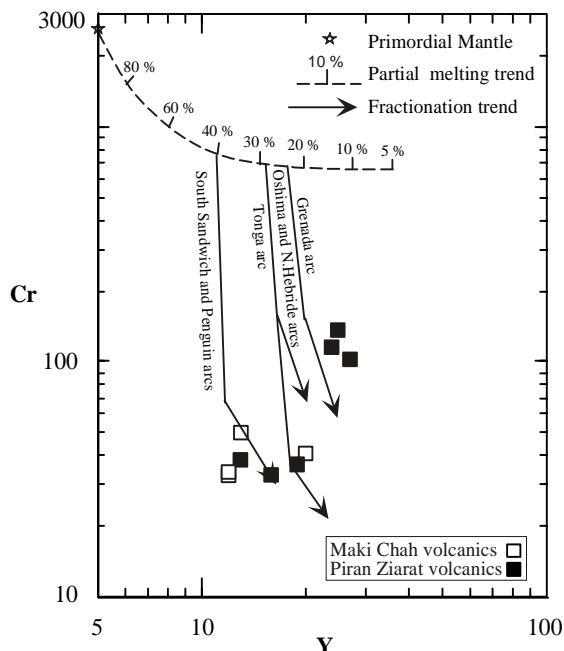


Fig. 11. Cr versus Y plot (Pearce, 1982) for the Paleocene Volcanic rocks from the Chagai Arc.

(Rollinson, 1993). The $^{87}\text{Sr}/^{86}\text{Sr}$ ratio is determined for one sample (Rp-3) from Paleocene volcanic rocks of the Chagai Arc is 0.70446. This ratio is well below the reported ratios for Bulk earth (0.7052). The magmas with $^{87}\text{Sr}/^{86}\text{Sr}$ ratios less than the Bulk Earth value are considered to have been derived from a depleted mantle source (Wilson, 1989).

The $^{87}\text{Sr}/^{86}\text{Sr}$ ratio data from Paleocene volcanic rock of the Chagai arc is also plotted (Fig. 12) with a number of oceanic and continental margin type island arcs of the world. These include Tonga (Ewart *et al.*, 1977), Mariana (Gill, 1981), Kohistan (Peterson and Windley, 1991), New Briton (Woodhead and Johnson, 1993), Aleutian (Gill, 1981), Java (McDermott and Hawkesworth, 1991), New Zealand (Ewart *et al.*, 1977), Andes (Hawkesworth *et al.*, 1982) and average of many oceanic island arcs (Wilson, 1989). The $^{87}\text{Sr}/^{86}\text{Sr}$ values of N-MORB (Sun and McDonough, 1989) and Sub-oceanic lithosphere (Vance *et al.*, 1989) are also plotted in the same fig. The $^{87}\text{Sr}/^{86}\text{Sr}$ data closely correlate and plot with oceanic island arcs rather than continental margin type Arcs. The Paleocene volcanic rocks from the Chagai Arc has slightly higher $^{87}\text{Sr}/^{86}\text{Sr}$ than those of N-MORB and plot within the range of sub-oceanic lithosphere, which suggests the role of depleted sub-oceanic lithosphere in generation of the parent magma of the Paleocene volcanic rocks of the Chagai Arc.

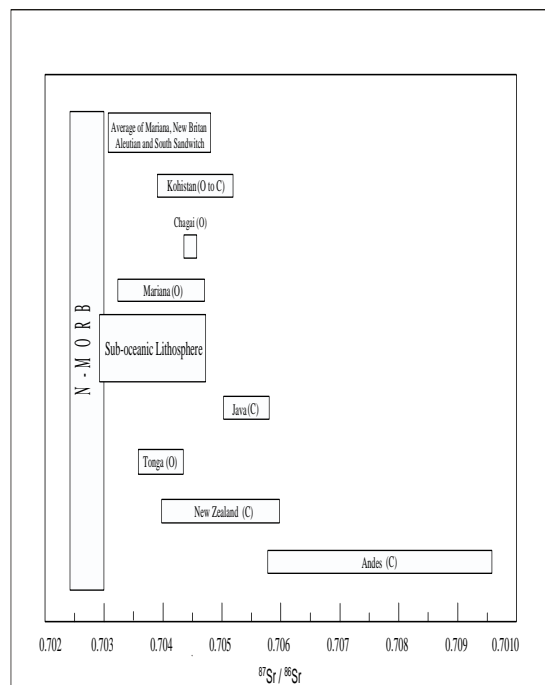


Fig. 12

Fig. 12. A comparison of Sr isotope ratios of the Paleocene volcanic rocks from the Chagai Arc with different island arcs of the world. (C) is for continental margin arcs and (O) is for oceanic island arcs respectively.

6. Conclusions

The Paleocene volcanic rocks from the Chagai Arc exhibit well-developed porphyritic texture: a common feature developed in the volcanic rocks found in island arcs (Ewart, 1982; Wilson, 1989). The petrogenetic studies suggest that these rocks are tholeiitic in nature and formed in an oceanic island arc rather than a continental margin type (Andean type) Arc. HFSE, REE contents and $^{87}\text{Sr}/^{86}\text{Sr}$ ratio indicate that parent magma of both the volcanic groups was derived from a depleted mantle source. The Piran Ziarat volcanics show higher values of Mg # and higher contents of Cr, Co and Ni as compared to Maki Chah Volcanics, which suggests that the former volcanics were derived from a more depleted magma source. The Piran Ziarat Volcanics generally exhibit progressively higher concentrations of LIL elements, and higher LIL/HFS element ratios relative to Maki Chah Volcanics, which suggest that the former Volcanics are more fractionated in nature. The parent magma of these rock suites was generated by about 15 to 30% partial melting of a depleted sub-arc mantle source and fractionated in upper level magma chamber.

7. Acknowledgements

Thankful to authors N. Brothers and A. Mateen J. K. (ed) Trench publisher for granting permission Fig. 5 and 6 A. Streckeisen for Table 3

(from A. Woodhead J.D We are highly indebted to Dr. Imran Ahmad Khan, Director General, Geological Survey of Pakistan (GSP), Mr. S. Hasan Gauhar, ex-Director General, GSP and Mr. Tahir Karim Director of the same Department for their support during field and laboratory research. Dr. T. Shirahase, ex-Director, Geological Survey of Japan (GSJ), Dr. M. Nakajima and Dr. M. Mikoshiba are greatly acknowledged for their guidance and help during Sr. isotope and REE analyses respectively in Geochemical Laboratory of GSJ).

References

- Ahmed, M. U. (1984) Geological exploration and preliminary evaluation of Dasht-e-Kain porphyry copper-molybdenum prospect Chagai district, Balochistan, Pakistan. Ph.D. Thesis (unpublished), Univ. Belgrade, Yugoslavia.
- Arthurton, R. S., G. S. Alam, S. A. Ahmed and S. Iqbal, (1979) Geological history of Alam Reg - Mashki Chah area, Chagai District, Balochistan. *In* Farah, A. and DeJong, K. A., (eds.), *Geodynamics of Pakistan*. Geol. Surv. Pakistan, 325-331.
- Arthurton, R. S., A. Farah, and W. Ahmed, (1982) The Late Cretaceous-Cenozoic history of western Balochistan, Pakistan - the northern margin of the Makran subduction complex. *In* Leggett, J. K., (ed.), *Trench Fore-Arc Geology*. Geol. Soc. London, Spec. Pub., (10): 343-385.
- Bakr, M. A. and R. O. Jackson, (1964) Geological Map of Pakistan. Geol. Surv. Pakistan, Quetta.
- Britzman, L. (1979) Fission track ages of intrusives of Chagai District, Balochistan, Pakistan. M.A. Thesis (unpublished), Dartmouth College, Hanover, N. H., U.S.A.
- Dykstra, J. D. (1978) A geol. study of Chagai Hills Balochistan, Pakistan using LANDSAT digital data. Ph.D. Thesis (unpublished), Dartmouth College, Hanover, N. H., U.S.A.
- Ewart, A., R. N. Brothers, and A. Mateen, (1977) An outline of the geology, geochemistry and the possible petrogenetic evolution of the Tonga-Kermadec- New-Zealand Arc., *Jr. Volcano. Gechem. Res.*, (2): 205-250.
- Ewart, A. (1982) The mineralogy and petrology of Tertiary-Recent orogenic volcanic rocks with special reference to andesitic-basaltic compositional range, *In* Throp, R. S., (ed.), *Andesites: Orogenic andesites and related rocks*. John Wiley and Sons, New York, 26-87.
- Farah, A., G. Abbas, K. A. DeJong and R. D. Lawrence, (1984) Evolution of the Lithosphere in Pakistan. *Tectonophysics*, (105): 207-227.

- Farah, A., R. D. Lawrence, and K. A. DeJong (1984) An overview of the tectonics of Pakistan, *In* B. U. Haq, and J. D. Milliman, (eds.), Marine geology and oceanography of Arabian Sea and coastal Pak. Van Nostrand Reinhold Company, New York, 161-176.
- Fyfe, W. S. (1976) Hydrosphere and continental crust. *Geosci. Can.*, (3):255-268.
- Gill, J. B. (1981) Orogenic Andesites and Plate Tectonics. Springer, Berlin, Pp.189.
- Govindaraju, K. (1989) Geostandards Newsletter, Special Issue, Working Group on Analytical standards of minerals, ores and rocks. France, (13): Pp.114.
- Gradstein, F. M., J. G. Ogg, A. G. Smith, F. P. Agterberg, W. Bleeker, R. A. Cooper, V. Davydov, P. Gibbard, L. Hinnov, M. R. House, L. Lourens, H. P. Luterbacher, McArthur, M. J. Melchin, L. J. Robb, J. Shergold, M. Villeneuve, B. R. Wardlaw, J. Ali, H. Brinkhuis, F. J. Hilgen, J. Hooker, R. J. Howarth, A. H. Knoll, J. Lasker, S. Monechi, J. Powell, K. A. Plumb, I. Raffi, U. Rohi, A. Sanfilippo, B. Schmitz, N. J. Shackleton, G.A. Shields, H. Strauss, J. Van Dam, T. Van Kolschoten, J. Veizer, and D. Wilson, (2004) *A Geo. Time Scale 2004*; Columbia Univ. Press New York.
- Hawkesworth, C. J., M. Hammill, A.R. Gledhill, P. V. Calsteren and G. Rogers, (1982) Isotope and trace elements evidence for late stage intra-crustal melting in the high Andes. *Earth Planet. Sci. Lett.*, (58): 240-254.
- Hole, M. J., A. D. Saunderson, G. F. Marriner, and J. Tarney, (1984) Subduction of pelagic sediments; implication for the origin of Ce-anomalous basalts from Mariana Islands. *Jour. Geol. Soc. London*, (141): 453-472.
- Hunting Survey Corporation Limited, (1960) Reconnaissance Geology of Part of West Pakistan. A Colombo Plan Cooperative Project, Govt. of Canada, Toronto, Canada, Pp. 550.
- Imai, N., (1990) Multielement analysis of rock with the use of geological certified reference materials by inductively coupled plasma mass spectrometry. *Analytical Science*, (6): 389-385.
- Jakes, P. and J. R. White, (1972) Major and trace elements abundances in volcanic rocks of organic areas. *Bull. Geol. Soc. Am.*, (83): 29-40.
- Jones, A. G. (1960) Reconnaissance Geology of Part of West Pakistan. A Colombo Plan Cooperative Project, Govt. of Canada, Toronto, (Hunting Survey Corporation report) Pp.550.
- Kazmi, A. H. and M. Q. Jan, (1997) Geology and Tectonics of Pakistan. Graphics Publishers, Kar. Pakistan, Pp.554.
- Kazmin, V. G. (1991) Collision and rifting in the Tethyan Ocean: geodynamic implications. *Tectonophysics*, (196): 371-384.
- Khan, M. A., R. J. Stern, R. F. Gribble, and B. F. Windley, (1997) Geochemical and isotopic constraints on subduction polarity, magma source and paleogeography of the Kohistan intra-oceanic arc, northern Pakistan Himalaya. *Jour. Geol. Soc. London*, (154): 935-946.
- Le Bas, M. J., R. W. Le Maitre, A. Streckeisen, and B. Zanettin, (1986) A chemical classification of volcanic rocks based on the total alkali silica diagram. *Jour. Petrol.*, (27): 745-750.
- Masuda, A. (1968) Geochemistry of Lanthanides in basalts of central Japan. *Earth Planet. Sci. Lett.* (4): 284-292.
- McDermott, F. and C. J., Hawkesworth, (1991) Th, Pd and Sr isotope variations in young arc volcanic and oceanic sediments. *Planet. Sci. Lett.*, (104): 1-15.
- Melson, W. T., G. Thompson, and T. H. Van Andel, (1968) Volcanism and metamorphism in the Mid-Atlantic ridge 22°N Latitude. *Jour. Geophys. Res.*, (73): 5925-5941.
- Meschede, M. (1986) A method of discriminating between different types of mid-oceanic ridge basalts and continental tholeiites with the Nb-Zr-Y diagram, *Chem Geol.*, (56): 207-218.
- Metcalf, I. (1995) Gondwana dispersion and Asian accretion. *Jour. Geol.*, Series, B. 223-266.
- Miyashiro, A. (1974) Volcanic rock series in island arcs and active continental margins. *Am. Jour. Sci.*, (274): 321-355.
- Mullen, E. D. (1983) MnO/TiO₂/P₂O₅: A minor element discrimination for basaltic rocks of oceanic environments and its implications for petrogenesis. *Earth Planet Sci. Lett.*, (62): 53-62.
- Nakamura, N. (1974) Determination of REE, Ba, Fe, Mg, Na and K in carbonaceous and ordinary chondrites. *Geochim. Cosmochim. Acta.*, (38):757-775.
- Nigell, R. H. (1975) Reconnaissance of the geology and ore mineralization in part of the Chagai District, Balochistan, Pakistan. U. S. Geol. Surv., Project Report (PK-27), Pp. 550.
- Ogg, J. G., G. Ogg, and F. M. Gradstein, (2008) The Concise Geological Time Scale, International Commission on Stratigraphy (www.stratigraphy.org).
- Pearce, J. A. and J. R. Cann, (1973) Tectonic setting of basic volcanic rocks determined using trace elements analysis. *Earth Planet Sci. Lett.*, (19):290-300.

- Pearce, J. A. and M. Norry, (1979) Petrogenetic implications of Ti, Zr, Y and Nb variation in volcanic rocks. *Cont. Mineral. and Petrol.*, (**69**): 33-47.
- Pearce, J. A. (1982) Trace elements characteristics of lavas from destructive plate boundaries. *In* R. S. Throp, (ed.), *Andesites: Orogenic andesites and related rocks*. John Wiley and Sons, New York, 525-548.
- Pearce, J. A. (1983) The role of subcontinental lithosphere in the magma genesis at destructive plate margin, *In* C. J. Hawkes-worth, and M. J., Norry, (eds.), *Continental basalts and mantle xenoliths*. Natwich Shiva, 230-249
- Perello, J., A. Raziq, J. Schloderer, and A. U. Rehman, (2008) The Chagai Porphyry Copper Belt, Baluchistan Province, Pakistan. *Eco. Geol.*, (**103**):1583-1612.
- Petterson, M. G., and B. F. Windley, (1985) Rb-Sr dating of the Kohistan arc batholith in the Trans-Himalayan of north Pakistan and tectonic implications. *Earth Planet. Sc. Lett.*, (**74**): 45-57.
- Rollinson, H. (1993) *Using Geochemical data: evaluation, presentation, interpretation*, John Wiley and Sons, New York.
- Saunders, A. D. and J. Tarney, (1979) The geochemistry of basalts from a back-arc spreading centre in the east Scotia Sea. *Geochem. Cosmochem. Acta.* (**43**): 555-572.
- Saunders, A. D. and J. Tarney, (1991) Back-arc basins. *In* Floyd. P.A. (ed.), *Oceanic Basalts*, Blackie, London, 219-263.
- Shervais, J. W. (1982) Ti versus V plots and the petrogenesis of modern and ophiolitic lavas. *Eart Planet Sc. Lett.*, (**59**): 101-108.
- Siddiqui, R. H., W. Khan, and M. Haque, (1986) Petrological and petrochemical studies of northcentral Chagai Belt and its tectonic implications. *Acta Mineralogica Pakistanica*, (**2**): 12-23.
- Siddiqui, R. H., S. A. Hussain, and M. Haque, (1987) Geology and petrography of Eocene mafic lavas of Chagai island arc, Balochistan, Pakistan. *Acta Mineralogica Pakistanica*, (**3**): 123-128.
- Siddiqui, R. H., M. Haque, and S. A. Hussain, (1988) Geology and petrography of Paleocene mafic lavas of Chagai island arc, Balochistan, Pakistan. *Geol. Surv. Pak., I. R.*, (**361**): Pp.18
- Siddiqui, R. H. (1996) Magmatic evolution of Chagai-Raskoh arc terrane and its implication for porphyry copper mineralization. *Geological*, (**2**): 87-119.
- Siddiqui, R. H. (2004) Crustal evolution of the Chagai-Raskoh arc terrane, Balochistan, Pakistan. Unpublished PhD Thesis, Centre of Excellence in Geology, University of Peshawar, Pakistan.
- Siddiqui, R. H., M. A. Khan, and M. Q. Jan (2005) Petrogenesis of Eocene Lava flows from the Chagai Arc, Balochistan, Pakistan and its tectonic implications. *Geol. Bull. U. of Peshawar* (**38**): 163-187.
- Sillitoe, R. H. (1978) Metallogenic evolution of a collision mountain belt in Pakistan: a preliminary analysis. *Jour. Geol. Soc. London*, (**125**): 377-387.
- Spector, A. and Associates Ltd., (1981) Report on interpretation of aeromagnetic survey data, Balochistan Province, Pakistan. Project Report **J-223**, Pp.107.
- Stocklin, J. (1974) Possible ancient continental margin in Iran. *In* C.I. Burk, and C.L., Drake,(eds.), *Geology of Continental Margins*. Springer, New York, 889-903.
- Stoneley, R. (1974) Evolution of a continental margin bounding a former southern Tethys, *In* C. I. Burk, and C. L., Drake, (eds.), *The Geology of Continental Margins*. Springer, New York, 873-887.
- Sun, S. S. and W. F. McDonough, (1989) Chemical and isotopic systematics of ocean basalt, implication for mantle composition and processes. *In* A. D Saunders, and M. J., Torny, (eds.), *Magmatism in the ocean basins*. *Geol. Soc. London, Spec. Pub.*, (**42**): 313-345.
- Taylor, S. R. and S. M. McLennan, (1985) *The continental crust: its composition and evolution*. Blackwell, Oxford.
- Vredenburg, E. W. (1901) A geological sketch of the Balochistan desert and part of Eastern Persia. *Geol. Surv. India, Mem.*, Pp.302.
- Wilson, M. (1989) *Igneous Petrogenesis*. Unwin and Hyman, London, Pp.466.
- Winchester, J. A. and P. A. Floyd, (1977) Geochemical discrimination of different magma series and their differentiation products using immobile elements: *Chemical Geology*, (**20**): 325-343.
- Woodhead, J. D. and R. W. Johnson, (1993) Isotope and trace elements profiles across the New Britain island arc, Papua, New Guinea. *Cont. Mineral. Petrol.*, (**113**): 479-491.
- Woodhead, J. D. (1988) The origin of geochemical variations in Mariana lavas. A general model for petrogenesis in intra oceanic island arc. *Jour. Petrol.*, (**29**): 805-830.
- Wyllie, P. J. (1982) Subduction products according to experimental predictions. *Bull. Geol. Soc. Am.*, (**93**): 468-476.

